International Journal of GEOMATE, Dec., 2018 Vol.15, Issue 52, pp.129-136
Geotec., Const. Mat. & Env., DOI: https://doi.org/10.21660/2018.52.29740
ISSN: 2186-2982 (Print), 2186-2990 (Online), Japan

THE RESPONSE OF PILES UNDER TENSION LOADS BASED ON ANALYTICAL METHOD AND FINITE ELEMENT ANALYSIS

*Kelvin Lo[1], Dominic Ong[1] and Erwin Oh[1]

[1] Griffith School of Engineering and Built Environment, Griffith University, Australia

*Corresponding Author, Received: 07 Aug. 2018, Revised: 30 Aug. 2018, Accepted: 05 Oct. 2018

ABSTRACT: In the past, there were many research studies carried out on the response of single piles and pile groups under compression loads, but it was comparatively lesser for piles and pile groups under uplift loads. Uplift loads on piles usually occur in pile foundations supporting wind farm structures, tall chimneys, transmission towers and jetty structures. During recent decades, research studies on piles under uplift loads have progressed, and were mainly focused on the capacity, failure modes and load displacement performance of single piles, but no research has been done on the influence zone of a pile and its effects within a group. This paper presents the initial findings of research to investigate the stress distribution and influence zone of a single pile under uplift loads using a hybrid approach combining analytical theory and 2D Finite Element (FE) analysis. Finally, the effect of the estimated influence zone was successfully verified in 3D FE analysis which confirmed that group efficiency reduced when an adjacent pile was within the estimated influence zone and thus piles behave as a group.

Keywords: Piles, Soil stress, Influence zone, Uplift loads

1. INTRODUCTION

Pile-soil interaction, soil stress around piles and the extent of the influence zone under uplift loading are still not clearly understood, although many research studies have been done on piles. The mechanism is important as it affects the group efficiency and interaction between piles within a group. Stress distribution in the soil mass surrounding a pile, the extent of the influence zone, and the combined shape of a group under uplift loads have been investigated by a hybrid approach combining analytical method under concentric cylindrical theory and 2D FE analysis. 3D FE analysis confirmed that group efficiency reduces when an adjacent pile is within the estimated influence zone, and the piles behave as a group. Initial findings of this research are presented in this paper.

2. BACKGROUND

2.1 Uplift Capacity

The limiting frictional approach is the universal approach followed to evaluate the uplift resistance of piles [1]. Several empirical equations were developed to estimate the uplift capacity of single piles such as [2-5]. Meyerhof [3] introduced an uplift coefficient to the skin friction parameters assuming the failed soil mass under the axial pull of a pile had a roughly similar shape as for a shallow anchor. For a fixed value of pile friction angle, average skin friction was observed to increase with the slenderness ratio (L/d, length to diameter) up to a limiting value and thereafter it remains constant. Das [4] also observed the average skin friction reaches a constant value at a critical L/d ratio and this critical depth ratio is dependent on relative density.

2.2 Pullout Failure Modes

In recent years, several pull-out failure modes of single piles have been proposed using analytical, semi-empirical and experimental methods to estimate the uplift capacity of single piles. Failure modes can be grouped into four categories and they are cylindrical shear, truncated cone, curved surface, and the combination of cylindrical shear with breakout cone. All these represent individual cases, but no conclusion has been made as a completed scenario so far, and some are even not quite consistent with each other. The analytical methods include [6-8] which based on an assumption that the mobilized failure surface is log spiral, curve or cone frustum in shape to predict the uplift capacity. Experimental tests were conducted by [9, 10]. Semi-empirical approaches combining theoretical and experimental methods were performed by [11, 12] assuming the slip surface as a truncated inverted cone. Based on the above research work, it is noted that the pile-soil interaction, the coefficient of earth pressure, pile slenderness ratio, and body of revolution of surrounding soil are the important factors to influence the pile response and load capacity under uplift loads. Sowa [2] commented the accuracy would mainly depend on the correctness of the adopted value of the coefficient of earth pressure.

2.3 The Effects of Influence Zone

Bowles [13] suggested the soil pressures produced from either side friction or point bearing will overlap. The superimposed pressure density will depend on both the pile load and spacing, and if sufficiently large the soil will fail in shear or the settlement will be excessive. He observed the stress intensity in the overlapping stress zone will obviously decrease with increase in pile spacing. Meyerhof and Adams [14] conducted uplift tests on small groups of circular footings and shafts. They suggested the resistance of soil uplift is a combination of the soil weight and mobilized shear resistance within a defined boundary or failure surface. Lee, Kim, Sim, Kim and Lee [15] conducted field pull-out tests and proposed formulas for group efficiency in compression ground anchor related to the zone of influence cone and borehole diameter. Habib [16] inferred the influence zone under loading affects the group efficiency. Tan, Dasari and Lee [17] commented on the zone of influence under pulling affects the choice of 2D and 3D analyses. All these researchers emphasize the importance of the influence zone and soil behavior around the pile to affect the group behavior.

2.4 Influence Zone And Stress Distribution Under Compression

For pile under compression loads, there are already some researchers [18-20] using the analytical method and FE analysis to investigate the extent of the influence zone of a pile under compression loads. Randolph and Wroth [18] used concentric cylindrical theory in shear to idealize the soil deformation around a pile shaft to investigate the stress distribution in the surrounding soil mass, and the load transfer method to investigate the pile response under compression loads. It assumes the soil displacement due to the pile loads is predominantly vertical, and that radial displacement is negligible. They compared the results of the analytical method to the integral equation and FE analysis in homogenous and non-homogenous linear-elastic soils and predicted the extent of the influence zone (only for L/d = 40) under compression loads. A number of researchers have shown that the concentric cylindrical approach is a good approximation of the deformation patterns from more rigorous analyses such as FE analysis [21]. Guo and Randolph [19] continued the work to use a "hybrid" approach which utilized FE analysis to back-figure the extent of the influence zone in the analytical equations for non-homogenous soil under compression loads. Guo [20] further developed a closed form solution for the load-displacement behavior of a pile under compression loads in non-homogenous soil with initial shear modulus at the ground surface. All this research work is under compression loads, but not much work has been carried out for uplift loads. Little research was conducted on pile response under uplift forces [22]. The studies on the uplift capacity of pile groups embedded in the sand are scanty [23, 24].

2.5 Influence Zone And Stress Distribution Under Tension

Recently, several researchers such as [25-27] adopted load transfer method under nonlinear, hyperbolic and softening skin friction models to estimate the load-displacement response of single piles, but not much discussion on the extent of the influence zone. Only [26] recommended using percentage in shear stress ratio to decide the space needed between two anchor piles. Influence zone factors (r_m or r_e) were used in [28-31] to predict the load-displacement response of piles, but the adopted influence zone factors were based on previous research for pile under compression loads. van Baars and van Niekerk [32] mentioned that the surrounding soil stress is reduced due to the uplift of the soil mass surrounding the piles during loading of tension piles. The principal stress rotation is different under compression and tension loads.

For piles under uplift loads, there is no detailed publication to investigate the stress distribution in the surrounding soil mass, influence zone, interaction mechanism within a pile group, and the combined shape of the pile group during loading, when this submission is being prepared. All these are still not clearly understood. It is therefore important to understand the mechanism to improve the efficiency and accuracy in engineering solutions and provide competence judgment on the use of two-dimensional models.

3. HYBRID APPROACH

This research proposes to adopt a "hybrid" approach using analytical theory combining FE analysis. The extent of the influence zone is back-figured by fitting the results of FE analysis to the analytical method. Shear stress and vertical displacement along the pile shaft from FE analysis are fed into concentric cylindrical equations. The shear stress and vertical displacement in surrounding soil mass along the radial distance under concentric cylindrical theory are compared to the results of FE analysis by adjusting an influence zone number in the concentric cylindrical equation.

3.1 Concentric Cylindrical Theory

The analytical approach is based on the concentric cylindrical theory which is originally from [18]. The deformation of the soil around a pile at depth z under uplift movement may be idealized in Fig. 1, assuming

upward direction is positive.

Considering the vertical force equilibrium of a soil element in Eq. (1) and ignoring the second-order terms, Eq. (2) is obtained.

$$-\left(\tau\frac{\partial\tau}{\partial r}dr\right)(r+dr)d\theta dz+\tau r d\theta dz-\left(\sigma_z+\frac{\partial\sigma_z}{\partial z}dz\right)\left(r+\frac{dr}{2}\right)d\theta dr+\sigma_z\left(r+\frac{dr}{2}\right)d\theta dr=0 \quad (1)$$

$$\frac{\partial(\tau r)}{\partial r}+r\frac{\partial\sigma_z}{\partial z}=0 \quad (2)$$

where τ is the induced shear stress, σ_z is the induced vertical stress, r is the radial distance from the pile center, and z is the distance above the pile toe.

Since the increase in shear stress in the vicinity of the pile shaft will be much greater than the increase in vertical stress, similar to [18], the second term of Eq. (2) is ignored and it becomes:

$$\tau_r(z)=\frac{r_0\tau_0(z)}{r} \quad (3)$$

where $\tau_r(z)$ is the induced shear stress in soil mass at the radial distance (r) from the pile center and distance (z) above the pile toe, $\tau_0(z)$ is the induced shear stress at the shaft at distance (z) above the pile toe, and r_0 is the pile radius.

Similar to [18], assuming the primary displacement being vertical and integrating the displacement of the surrounding soil mass from an estimated radius (r_m) at which the shear stress becomes negligible, the induced vertical displacement in the soil mass will be:

$$w_r(z)=\frac{\tau_0(z)r_0}{G}\ln\left(\frac{r_m}{r}\right) \quad (4)$$

where $w_r(z)$ is the induced vertical displacement in soil mass at the radial distance (r) away from the pile center and distance (z) above the pile toe, and G is the soil shear modulus.

The dimensionless vertical displacement profile along the radial distance is then:

$$\frac{Gr_o w_r(z)}{P_t}=\frac{Gr_o}{P_t}\left[\frac{\tau_0(z)r_0}{G}\ln\left(\frac{r_m}{r}\right)\right] \quad (5)$$

where P_t is the uplift load at the pile top.

3.2 Finite Element Analysis

A model having a small incremental upward displacement at the pile top was conducted under the Mohr-Coulomb (MC) model in PLAXIS 2D axis-symmetric analysis. The radius (r) and length (L) of the pile are 0.15m and 4.5m respectively. PLAXIS 3D analysis has also been conducted to verify the effects of the influence zone between two piles. The pile and soil parameters are summarized in Table 1.

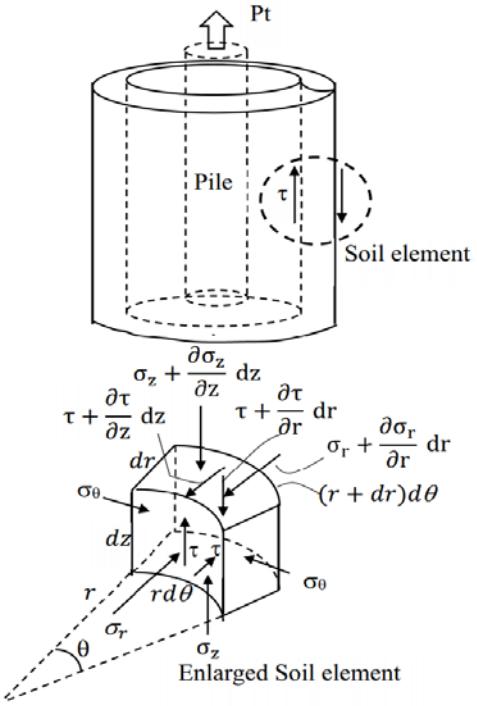

Fig.1 Shear deformation model of the soil around a pile in tension (modified from [18])

Table 1 Summary of the pile and soil parameters

	Model	**c** (kPa)	ϕ (°)	υ_s	E(kPa)
Soil	MC	1	30	0.3	1E4 + 1000 z
	Model	E(kPa)	υ_p	L(m)	r (m)
Pile	Note 2	$3x10^7$	0.15	4.5	0.15

Note 1: c is the soil cohesion, ϕ is the soil friction angle, G is the soil shear modulus, υ_s is the soil Poisson ratio, E is the pile modulus, υ_p is the pile Poisson ratio, L is the pile length, r is the pile radius.
Note 2: Linear-elastic model in the 2D model and embedded beam element in the 3D model.

The 2D and 3D models are shown in Figs. 2 and 3 respectively. The vertical and horizontal extents of the models are 7.5m and 10m respectively.

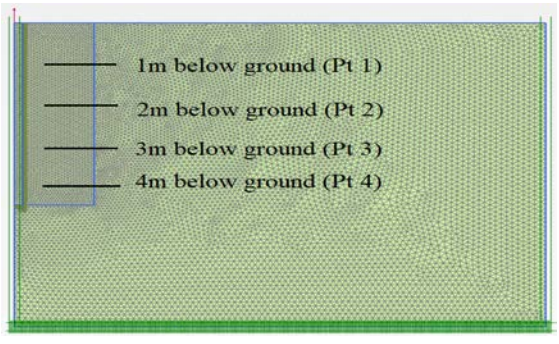

Fig.2 PLAXIS 2D axis-symmetry model.

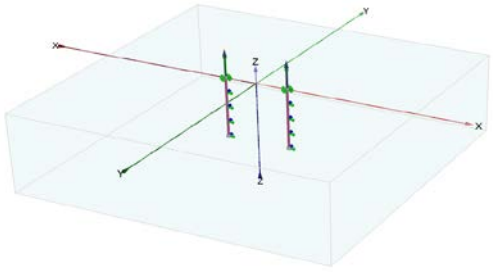

Fig.3 PLAXIS 3D model.

4. RESULTS AND DISCUSSIONS

4.1 0.5mm Upward Displacement At The Pile Top

At 0.5mm upward displacement at the pile top, the induced shear stress along the radial distance away from the pile center are shown in Figs. 4-7 (1.0m, 2.0m, 3.0m and 4.0m below ground respectively). The results of the analytical method generally agree with the FE analysis (PLAXIS) with less than 5 % difference (Table 2), except the zone around the pile toe (i.e. 4.0m below ground). Equations (2) and (3) in the analytical theory assume $\frac{\partial(\tau r)}{\partial r}$ to be zero. However, at 4.0m below ground, $\frac{\partial(\tau r)}{\partial r}$ already deviates away from zero (negative) starting at r = 0.25m (see Table 3) and the assumption of Eq. (3) in the analytical theory is no longer valid.

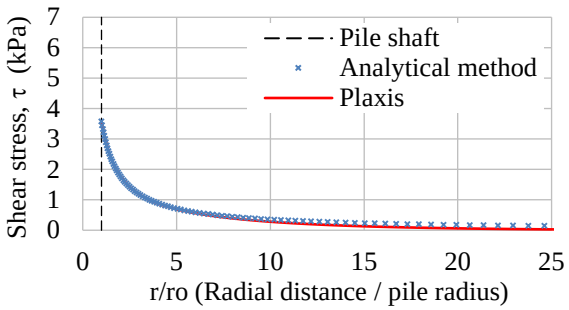

Fig.4 Shear stress along the radial distance away from the pile (1.0m below ground)

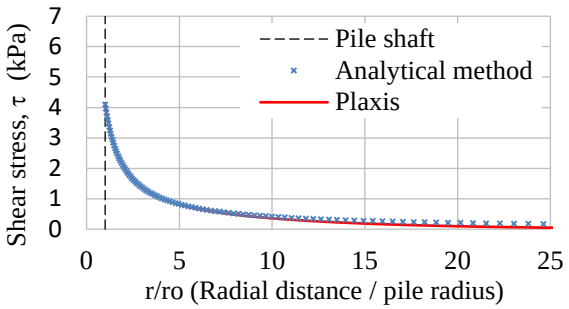

Fig.5 Shear stress along the radial distance away from the pile (2.0m below ground – around the mid-depth section of the pile)

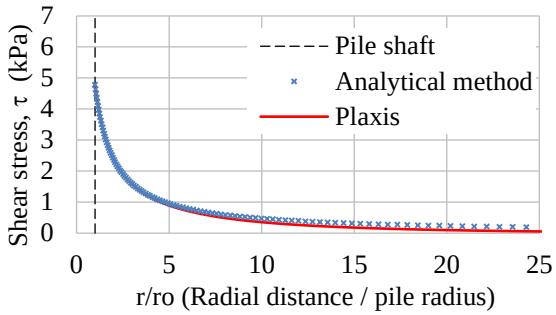

Fig.6 Shear stress along the radial distance away from the pile (3.0m below ground)

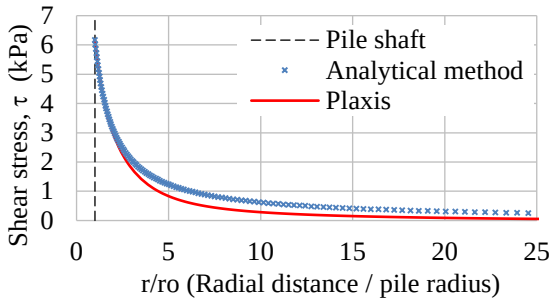

Fig.7 Shear stress along the radial distance away from the pile (4.0m below ground)

In Table 2, the best-agreed outcomes between the analytical method and FE analysis is around the mid-depth section of the pile (i.e. Pt ref. =2, at 2.0m below ground), which is considered the least influenced from the boundaries (discontinuities at the pile top and toe). Similar to [18], the vertical displacement profile around the mid-depth section of the pile is shown in Fig. 8.

Table 2 Percentage difference to the induced shear stress (τ_o) at the pile shaft

Pt Ref. (τ_o, kPa)	r/r_o	Shear (kPa)		%
		Analytical	FEM	
1 (3.58)	5	0.72	0.69	0.84
	15	0.24	0.13	3.07
	25	0.14	0.03	3.07
2 (4.09)	5	0.82	0.81	0.24
	15	0.27	0.18	2.20
	25	0.16	0.05	2.69
3 (4.79)	5	0.96	0.89	1.46
	15	0.32	0.18	2.92
	25	0.19	0.05	2.92
4 (6.17)	5	1.23	0.78	7.29
	15	0.41	0.15	4.21
	25	0.69	0.06	10.2

Note: Pt Ref. refers to Fig. 2.

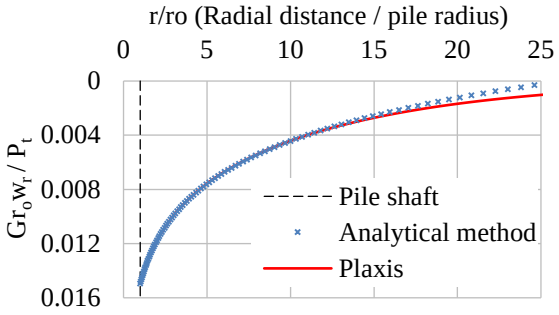

Fig.8 Dimensionless vertical displacement (Eq. 5) along the radial distance away from the pile (2.0m below ground)

Table 3 Change in shear and vertical stress in FE

r (m)	Pt Ref.	$r\frac{\partial\sigma_z}{\partial z}$	$\frac{\partial(\tau r)}{\partial r}$	$r\frac{\partial\sigma_z}{\partial z}+\frac{\partial(\tau r)}{\partial r}$
0.25	1.0	0.01	-0.02	-0.01
	2.0	0.00	0.00	0.00
	3.0	0.02	-0.02	0.00
	4.0	0.31	-0.46	-0.15
0.5	1.0	0.04	-0.05	-0.01
	2.0	0.02	-0.02	0.00
	3.0	0.09	-0.10	0.00
	4.0	0.63	-0.66	-0.04
0.75	1.0	0.08	-0.09	-0.01
	2.0	0.04	-0.04	0.00
	3.0	0.15	-0.16	-0.01
	4.0	0.45	-0.47	-0.02
1	1.0	0.12	-0.12	0.00
	2.0	0.08	-0.08	0.00
	3.0	0.18	-0.18	0.00
	4.0	0.30	-0.29	0.01
$\sum\frac{\partial(\tau r)}{\partial r}$		1m below ground	= - 0.26	
		2m below ground	= - 0.15	
		3m below ground	= - 0.47	
		4m below ground	= - 1.86	

Note: Negative implies decreasing; $\sum\frac{\partial(\tau r)}{\partial r}$ (within 1m radial distance); Pt Ref. refers to Fig. 2.

In Fig. 8, the results of the analytical and FE analysis agree well around the mid-depth section of the pile, which is similar to [18]. The value of r_m (the radial distance away from the pile center at which the shear stress becomes negligible) obtained in Eq. (4) is about 4.0m. In the FE analysis, the shear stress ratio ($\frac{\tau_{r=4}}{\tau_0}$) around the mid-depth section of the pile is about 1%. The shear ratio of 1% is taken as a reference point in this paper that the induced shear stress in the soil mass becomes negligible under the pulling action of the pile. This is in terms of the extent of the influence zone away from the pile center. Accordingly, the estimated extent of the influence zone away from the pile center is shown in Fig. 9, which is similar to [19]. Two FE sensitivity analyses have been carried out to assess the negligible effect of the boundary distance and mesh size. Table 4 shows the summary of the sensitivity analyses and Fig. 9 shows the negligible effect of the boundary distance and mesh size on the estimated extent of the influence zone. The extent of the influence zone is generally constant around the mid-depth section of the pile, except the top and toe sections of the pile. It can be explained by comparing the $\sum\frac{\partial(\tau r)}{\partial r}$ within 1m radial distance around the pile in Table 3 (Table 2 shows shear stress diminished about 80% within 1m radial distance, where is believed to be an important zone affecting the deformation behavior). The analytical theory assumes $\frac{\partial(\tau r)}{\partial r}$ equal to zero in Eq. (2) and Eq. (3). In Table 3, $\sum\frac{\partial(\tau r)}{\partial r}$ is the closest to zero around 2.0m below ground (mid-depth section), then continuously deviates away from zero (negative) when further up and down the pile. Negative means the decrease of τ is comparatively fast within a radial range, therefore the estimated extent of the influence zone reduces at the top and toe sections of the pile. The negative value of $\frac{\partial(\tau r)}{\partial r}$ is due to $\frac{\partial\sigma_z}{\partial z}$ being positive in order to maintain the force equilibrium in Eq. (2).

The upward movement of the pile body induces upward force which reduces the effective vertical stress of the surrounding soil mass, as explained in [32-35]. Higher shear stress is induced around the toe due to pile discontinuity, which results in a larger reduction in effective stress. Also, the shear stress decreases near the ground surface where the reduction in the effective vertical stress diminishes. These results in $\frac{\partial\sigma_z}{\partial z}$ being positive at the pile top and toe (z is positive in the upward direction from the pile toe).

Table 4 Details of the sensitivity analyses

Model	No. of soil elements	Element Size (m) Ave.	Element Size (m) Min.	Horiz. Extent (m)
1	20189	0.09	0.04	10
2	78463	0.05	0.02	10
3	15099	0.13	0.05	15

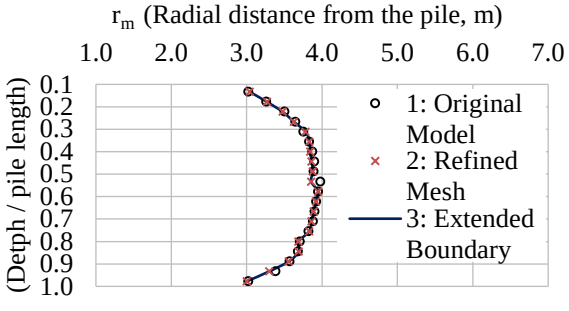

Fig.9 Influence zone in the sensitivity analysis

4.2 Models of 0.5mm, 1.0mm, 1.5mm and 2.0mm Upward Displacements At The Pile Top

The FE Models of 0.5mm, 1mm, 1.5mm and 2.0mm upward displacements at the pile top have been conducted. When increasing in upward displacement, a zone of plastic points (indicates plastic slip along the pile shaft) develops around the pile top and gradually extends down the pile. Plastic slip along the whole shaft occurs when upward displacement at about 1.7mm (about 1% diameter). The ultimate capacity of 59 kN is mobilized, which is very close to that calculated from [14].

The estimated extent of the influence zones for different upward displacements at the pile top obtained in the FE analysis are shown in Fig. 10. Figure 10 shows that the extent of the influence zones is changing when increasing the upward displacement at the pile top. Finally, an approximately truncated inverted cone is formed (i.e. the models of 1.5 and 2.0 mm upward displacements at the pile top, in which $\frac{\partial(\tau r)}{\partial r}$ becomes positive around the upper section of the pile). Figure 11 shows $\frac{\partial \sigma_z}{\partial z}$ becomes negative around the upper section of the pile, which results in $\frac{\partial(\tau r)}{\partial r}$ being positive in order to maintain the force equilibrium in Eq. (2). Positive $\frac{\partial(\tau r)}{\partial r}$ means the decrease of τ is comparatively slow within a radial range, which increases the estimated extent of the influence zone around the upper section of the pile. In Fig. 11 (the model of 1.5mm upward displacement at the pile top), the effective vertical stress in surrounding soil mass no longer reduces but increases around the upper section of the pile (zone of high plastic slip). Figure 12 shows that the soil layers in this zone move up relatively less comparing to the lower layers in 1.5mm upward displacement model. The lower layers force the upper layers to move up and therefore increase in effective vertical stress.

The shear stress distributions along the pile shaft for the models of 0.5mm to 2.0mm upward displacements at the pile top are shown in Fig. 13. In 1.0mm displacement model, the shear distribution along the pile shaft is similar to [18, 19]. Plastic slip occurs from the pile top down to 1.5m below ground, then shear stress slightly increases down the pile and rapidly increases around the pile toe. Further increase in upward displacement at the pile top (i.e. from 1.0mm to 1.5mm displacement models), further shear stress cannot be taken up in the slip zone and is transferred to the lower sections of the pile. The slip zone was pushing down the pile until the whole shaft becomes plastic at about 1.7mm upward displacement at the pile top.

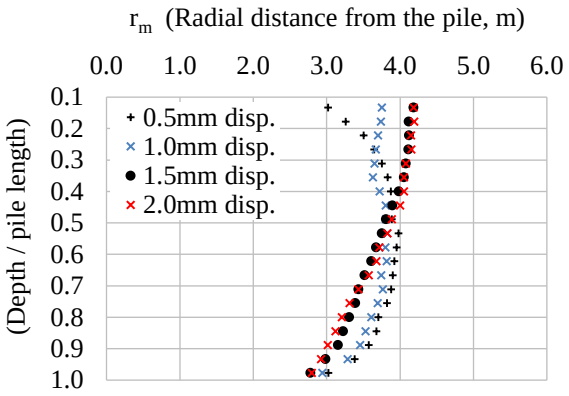

Fig.10 The estimated extent of the influence zones for different upward displacements at the pile top.

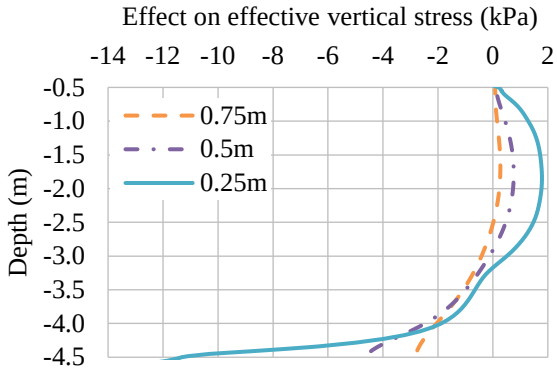

Fig.11 Effect on effective vertical stress at 0.25m, 0.5m and 0.75m radial distance from the pile (1.5mm upward displacement model).

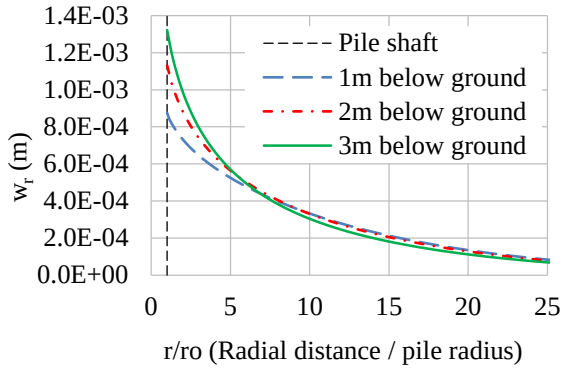

Fig.12 Soil vertical displacement at 1.0m, 2.0m, and 3m below ground (1.5mm upward displacement model).

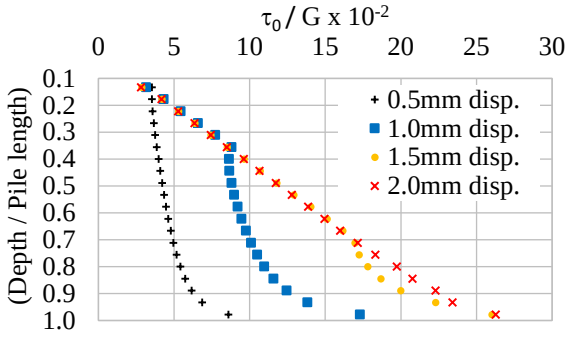

Fig.13 Shear stress distributions along the pile shaft at different upward displacements.

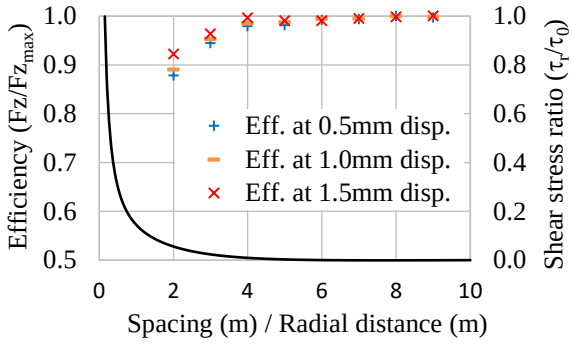

Fig.14 Left axis: Group efficiency against different pile spacing; Right axis: Shear ratio against the radial distance away from the pile.

4.3 3D Verification

The effect of the influence zone was investigated using PLAXIS 3D analysis comprising two identical piles using embedded beam elements in different pile spacing. The group efficiency (mobilized force / the summation of individual capacity) against different pile spacing is plotted in the left axis in Fig. 14. The right axis of Fig. 14 shows the shear ratio (mobilized shear stress/shear stress at the pile shaft) in the soil mass against the radial distance away from pile center, which demonstrates the effect of shear ratio on the group efficiency. The group efficiency obviously reduces when the pile spacing is less than the 4m influence zone where the shear ratio is still significant. It shows the close relationship between the shear ratio, the extent of the influence zone and group efficiency. In Figure 15, the behavior of individual pile is mobilized in 8m spacing where no interaction is observed, and group effect is mobilized when piles are spaced at 3m.

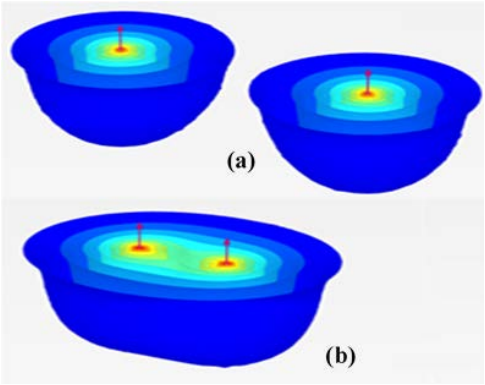

Fig.15 (a) Displacement contour (8m spacing); (b) Displacement contour (3m spacing).

5. CONCLUSIONS

This paper used a hybrid approach to estimate the extent of the influence zone and investigate the stress distribution in the soil mass surrounding a pile under uplifts loads. Results of 2D FE analysis was fed into the concentric cylindrical equations to estimate the extent of the influence zone, then the effect of the influence zone was successfully verified by 3D FE analysis. Effective vertical stress decreases under small loads, then increases around the plastic slip zone when approaching the ultimate capacity. The estimated extent of the influence zone is approximately a truncated inverted cone at the ultimate capacity. Digital Image Correlation (DIC) will be conducted to capture the strain field of soil mass surrounding the pile during upward loading to improve the FE models in the next part of this research.

6. REFERENCES

[1] Pise, P.J., Pile Foundations under Uplift Loads: An Overview, Indian Geotechnical Journal, Vol. 34(1), 2004.

[2] Sowa, V.A., Pulling Capacity of Concrete Cast in Situ Bored Piles, Canadian Geotechnical Journal, Vol. 7(4), 1970, pp. 482-493.

[3] Meyerhof, G.G., Uplift Resistance of Inclined Anchors and Piles, in Proc. 8th ICSMFE, Vol. 2, 1973, pp. 167-172.

[4] Das, B.M., A Procedure for Estimation of Uplift Capacity of Rough Piles, Soils and Foundations, Vol. 23(3), 1983, pp. 122-126.

[5] Kulhawy, F.H., Drained Uplift Capacity of Drilled Shafts, in Proc. 11th International Conference on Soil Mechanics and Foundation Engineering, 1985, pp. 1549-1552.

[6] Chattopadhyay, B.C., Pise, P.J., Uplift Capacity of Piles in Sand, Journal of Geotechnical Engineering, Vol. 112(9), 1986, pp. 888-904.

[7] Ghaly, A., Hanna, A., Ultimate Pullout Resistance of Single Vertical Anchors, Canadian Geotechnical Journal, Vol. 31(5), 1994, pp. 661-672.

[8] Su, Q., Zhang, X.X., Yin, P.B., Zhao, W.H., Ultimate Capacity Analysis and Determination of the Position

of Failure Surface for Uplift Piles, Mathematical Problems in Engineering, 2014.
[9] Das, S., Mukherjee, S., Venkatanarayana, P., Pull-out Resistance of Piles in Sand, Indian Geotechnical Conference (IGC-95), Vol. 1, 1995, pp. 173-177.
[10] Ghaly, A., Hanna, A., Model Investigation of the Performance of Single Anchors and Groups of Anchors, Canadian Geotechnical Journal, Vol. 31(2), 1994, pp. 273-284.
[11] Shanker, K., Basudhar, P.K., Patra, N.R., Uplift Capacity of Single Piles: Predictions and Performance, Geotechnical and Geological Engineering, Vol. 25(2), 2007, pp. 151-161.
[12] Hong, W.P., Chim, N., Prediction of Uplift Capacity of a Micropile Embedded in Soil, KSCE Journal of Civil Engineering, Vol. 19(1), 2015, pp. 116-126.
[13] Bowles, J.E., Foundation Analysis and Design, 5 ed., McGraw-Hill, New York, 1997, pp. 1007.
[14] Meyerhof, G.G., Adams, J.I., The Ultimate Uplift Capacity of Foundations, Canadian Geotechnical Journal, Vol. 5(4), 1968, pp. 225-244.
[15] Lee, S.W., Kim, T.S., Sim, B.K., Kim, J.S., Lee, I.M., Effect of Pressurized Grouting on Pullout Resistance and Group Efficiency of Compression Ground Anchor, Canadian Geotechnical Journal, Vol. 49(8), 2012, pp. 939-953.
[16] Habib, P., Recommendations for the Design, Calculation, Construction of Ground Anchorages, Balkema, the Netherlands, 1989.
[17] Tan, S.A., Dasari, G.R., Lee, C.H., Effects of 3d Discrete Soil Nail Inclusion on Pull-out, with Implications for Design, Proc. of the ICE-Ground Improvement, Vol. 9(3), 2005, pp. 119-125.
[18] Randolph, M.F., Wroth, C.P., Analysis of Deformation of Vertically Loaded Piles, Journal of Geotechnical and Geoenvironmental Engineering, Vol. 104(12), 1978.
[19] Guo, W.D., Randolph, M.F., Rationality of Load Transfer Approach for Pile Analysis, Computers and Geotechnics, Vol. 23(1-2), 1998, pp. 85-112.
[20] Guo, W.D., Vertically Loaded Single Piles in Gibson Soil, Journal of geotechnical and geoenvironmental engineering, Vol. 126(2), 2000, pp. 189-193.
[21] Pando, M.A., Ealy, C.D., Filz, G.M., Lesko, J.J., Hoppe, E.J., A Laboratory and Field Study of Composite Piles for Bridge Substructures, Federal Highway Administration, United States, 2006.
[22] Gaaver, K.E., Uplift Capacity of Single Piles and Pile Groups Embedded in Cohesionless Soil, Alexandria Engineering Journal, Vol. 52(3), 2013, pp. 365-372.
[23] Chattopadhyay, B.C., Uplift Capacity of Pile Groups, in Proc. 13th International Conference on Soil Mechanics and Foundation Engineering, Vol. 2, 1994, pp. 539-542.
[24] Patra, N.R., Pise, P.J., Uplift Capacity of Pile Groups in Sand, Electronic Journal of Geotechnical Engineering, Vol. 8, 2003.
[25] Xu, F., Zhang, Q.Q., Li, L.P., Wang, K., Zhang, S.M., He, P., Response of a Single Pile Subjected to Tension Load by Using Softening Models, Soil Mechanics and Foundation Engineering, Vol. 54(1), 2017, pp. 24-31.
[26] Xu, H.Y., Chen, L.Z., Deng, J.L., Uplift Tests of Jet Mixing Anchor Pile, Soils and Foundations, Vol. 54(2), 2014, pp. 168-175.
[27] Zhang, P., Yang, X.B., Wang, M., Difference Equation Solution of Nonlinear Single Piles Settlement Based on the Displacement Coordination, Electronic Journal of Geotechnical Engineering, Vol. 19, 2014, pp. 439-450.
[28] Zhang, Q.Q., Li, S.C., Zhang, Q., Li, L.P., Zhang, B., Analysis on Response of a Single Pile Subjected to Tension Load Using a Softening Model and a Hyperbolic Model, Marine Georesources & Geotechnology, Vol. 33(2), 2015, pp. 167-176.
[29] Zhu, B., Yang, M., Calculation of Displacement and Ultimate Uplift Capacity of Tension Piles, Journal of Building Structures, Vol. 3, 2006, pp. 015.
[30] Cheng, S., Zhang, Q.Q., Li, S.C., Li, L.P., Zhang, S.M., Wang, K., Nonlinear Analysis of the Response of a Single Pile Subjected to Tension Load Using a Hyperbolic Model, European Journal of Environmental and Civil Engineering, Vol. 22(2), 2018, pp. 181-191.
[31] Yao, W.J., Yuan, C.B., Chen, S.P., Analytical Solutions of Deformation of Anti-Pull Group Piles Considering Reinforcement Effect, Journal of Harbin Engineering University Vol. 38(10), 2017, pp. 1573-1579.
[32] van Baars, S., van Niekerk, W.J., Numerical Modelling of Tension Piles, International Symposium on Beyond 2000 in Computational Geotechnics, 1999, pp. 237-246.
[33] Ibrahim, A., Altahrany, A., Ashour, M., Pile Response under Axial Tension Forces in Sandy Soils, Journal of Bridge Engineering, Vol. 22(11), 2017.
[34] O'Neill, M.W., Side Resistance in Piles and Drilled Shafts, Journal of Geotechnical and Geoenvironmental Engineering, Vol. 127(1), 2001, pp. 3-16.
[35] De Nicola, A., Randolph, M.F., Tensile and Compressive Shaft Capacity of Piles in Sand, Journal of Geotechnical Engineering, Vol. 119(12), 1993, pp. 1952-1973.